Published in final edited form as:
Cell Metab. 2007 December ; 6(6): 446–457. doi:10.1016/j.cmet.2007.10.007.

Loss of Akt1 leads to severe atherosclerosis and occlusive coronary artery disease

Carlos Fernández-Hernando[1], **Eric Ackah**[1], **Jun Yu**[1], **Yajaira Suárez**[1], **Takahisa Murata**[1,3], **Yasuko Iwakiri**[1], **Jay Prendergast**[1], **Robert Q. Miao**[1], **Morris J. Birnbaum**[2], and **William C. Sessa**[1]

[1]Department of Pharmacology and Vascular Biology and Transplantation, Boyer Center for Molecular Medicine, Yale University School of Medicine, New Haven, Connecticut, USA.

[2]Department of Medicine, Howard Hughes Medical Institute, University of Pennsylvania School of Medicine, Philadelphia, Pennsylvania, USA.3

[3]Department of Veterinary Pharmacology, Graduate School of Agriculture and Life Sciences, The University of Tokyo, Tokyo, Japan.

SUMMARY

The Akt signaling pathway controls several cellular functions in the cardiovascular system; however, its role in atherogenesis is unknown. Here we show that the genetic ablation of Akt1 on an apolipoprotein E knockout background ($ApoE^{-/-}Akt1^{-/-}$) increases aortic lesion expansion and promotes coronary atherosclerosis. Mechanistically, lesion formation is due to enhanced expression of pro-inflammatory genes and endothelial cell and macrophage apoptosis. Bone marrow transfer experiments suggest that macrophages from $ApoE^{-/-}Akt1^{-/-}$ donors were not sufficient to worsen atherogenesis when transferred to $ApoE^{-/-}$ recipients suggesting that lesion expansion in the $ApoE^{-/-}$ $Akt1^{-/}$ strain may be of vascular origin. In the vessel wall, the loss of Akt1 increases inflammatory mediators and reduces eNOS phosphorylation suggesting that Akt1 exerts vascular protection against atherogenesis. The presence of coronary lesions in $ApoE^{-/-}$/ $Akt1^{-/-}$ mice provides a new model for studying the mechanisms of acute coronary syndrome in humans.

INTRODUCTION

Atherosclerosis is a chronic inflammatory process involving complex interactions of modified lipoproteins, monocyte-derived macrophages or foam cells, T lymphocytes, endothelial cells, smooth muscle cells, and fibroblasts (Glass and Witztum, 2001; Libby, 2002). The PI3K-Akt signaling pathway is involved in the regulation of cell metabolism, survival, migration, and gene expression in various cell types (Cantley, 2002; Whiteman et al., 2002). In the vascular wall, Akt has been shown to play an important role in the proliferation and migration of endothelial cells, regulation of vascular permeability and angiogenesis (Ackah et al., 2005; Chen et al., 2005; Phung et al., 2006). Recent studies of Akt knockout mice have shown that despite significant sequence homology, the three Akt isoforms have some non-redundant functions. While Akt1 deficient mice exhibit overall

Correspondence should be addressed to William C Sessa, william.sessa@yale.edu.

growth impairment (Chen et al., 2001; Cho et al., 2001b), Akt2 knockout mice have impaired glucose tolerance and insulin resistance (Cho et al., 2001a) and Akt3 nulls display a selective reduction in brain size (Easton et al., 2005; Tschopp et al., 2005). We have recently shown that Akt1 is an important Akt isoform expressed in endothelial cells, and that the loss of Akt1 results in reduced endothelial nitric oxide synthase (eNOS) phosphorylation, NO release, endothelial cell migration and impaired VEGF and ischemia-induced angiogenesis (Ackah et al., 2005). However, in vitro studies suggest that Akt1 may play either a pro-atherogenic or anti-atherogenic role. For example eNOS-derived NO has physiological properties that may be atheroprotective, including inhibition of apoptosis, smooth muscle cell proliferation, platelet aggregation and adhesion, and leukocyte activation and adhesion (Ignarro and Napoli, 2004; Kuhlencordt et al., 2001). However, PI3K-Akt activation may also enhances macrophage survival in lesions and persistent activation of Akt may promote cellular hypertrophy and hyperplasia, thereby promoting atherogenesis (Dzau et al., 2002; Shiojima et al., 2005). Since the integrative role of Akt1 in vivo is not described during atherogenesis, here we show that ApoE$^{-/-}$ Akt1$^{-/-}$ mice fed a high cholesterol diet exhibit markedly enhanced aortic atherosclerosis compared to littermates. More importantly, the absence of Akt1 leads extensive coronary atherosclerosis, a phenotype previously observed in mice lacking at least two components of the cholesterol metabolism (Braun et al., 2002; Caligiuri et al., 1999) or in apoE-deficient mice on Western-type diet for ten months (Nakashima et al., 1994; Reddick et al., 1994). The increased atherogenesis in mice lacking Akt1 is mechanistically linked to endothelial cell dysfunction and enhanced apoptosis in vascular cells.

RESULTS

Enhanced atherosclerosis and coronary occlusive lesions in absence of Akt1

To study the function role of Akt1 in atherogenesis, double knockout ApoE$^{-/-}$ Akt1$^{-/-}$ and corresponding ApoE$^{-/-}$ mice were subjected to a high cholesterol diet for 14 weeks and aortas were opened longitudinally and stained with Oil-Red O to visualize lipid rich, atherosclerotic plaques. As shown in Fig. 1a and 1b, the absence of Akt1 increased the number and size of aortic plaques. Lesion areas were greater particularly in the aortic arch (Fig. 1c) and thoracic aorta (Fig. 1d) compared to the abdominal region (Fig. 1e). In another cohort of mice, we quantified lesion areas in cross-sections of the aortic sinus. As shown in Fig. 1f, the loss of Akt1 increased the lesion area in the sinus compared to that observed in ApoE$^{-/-}$ mice. Moreover, we observed severe atherosclerosis in the coronary ostia, epicardial common coronary artery and intramyocardial branches (Fig. 1g, see Supplemental Fig. 1 for serial sectional analysis of coronary lesions) in all doubly mutant mice analyzed (n=12). This phenotype is atypical for ApoE$^{-/-}$ mice but can be in ApoE $^{-/-}$ mice found after feeding a Western diet for ten months (Nakashima et al., 1994; Reddick et al., 1994), in mice that lack both the LDL receptor and ApoE fed on a high cholesterol diet for 7 months (Caligiuri et al., 1999), SR-BI deficient mice bred on an ApoE$^{-/-}$ background (Braun et al., 2002) or ApoE$^{-/-}$ bred to mice transgenically expressing urokinase in macrophages (Cozen et al., 2004). Next, we confirmed occlusive coronary artery disease by ex vivo angiography (Fig. 1h). Thus, the genetic loss of Akt1 increases aortic and coronary atherogenesis. In addition to these coronary lesions observed in absence of Akt1, we also found a marked atherogenesis, and almost occlusive lesions, in the innominate/brachiocephalic artery of doubly mutant mice (Fig. 2). As a possible consequence of this accelerated atherosclerosis, we found significant mortality in ApoE$^{-/-}$Akt1$^{-/-}$ mice (5 of 22 animals died prior to the end of the feeding period whereas 0 of 42 ApoE$^{-/-}$ died).

Reduced body weight and no change in lipids in the absence of Akt1

Next, we examined multiple metabolic parameters of the mice. Body weights were significantly lower in the ApoE$^{-/-}$Akt1$^{-/-}$ versus ApoE$^{-/-}$ mice (Fig. 3a). Plasma triglycerides, cholesterol levels and lipoprotein profiles were similar in both groups before and after feeding a high cholesterol diet (Fig. 3b-d) indicating that the increase in lesion formation occurred independently of the plasma lipid profiles in the ApoE$^{-/-}$ Akt1$^{-/-}$double mutant mice.

Deletion of Akt1 decreases endothelial cell proliferation and viability

To determine the potential mechanisms of enhanced atherosclerosis in the double mutant mice, initially, we analysed Akt1 protein expression in cells traditionally associated with the development of atherosclerosis; endothelial cells (EC), vascular smooth muscle cells (VSMC) and monocytes. As seen in Fig. 4a, in all cells types examined, Akt1 is the major isoform expressed. One classic hypothesis of atherogenesis has suggested that “dysfunction” of ECs is an important early event for the development of atherosclerosis (Littlewood and Bennett, 2003; Tricot et al., 2000) and sites where plaques develop may be associated with impaired EC function and apoptosis. To investigate whether Akt1 is important for regulating EC proliferation and viability, we analysed EC proliferation at different time points and hypodiploid cells by flow cytometry. As shown in Fig. 4b, EC isolated from Akt1$^{-/-}$ mice did not grow as well as cells isolated from WT mice. Furthermore, the reintroduction of Akt1 (by retrovirus) into Akt1$^{-/-}$ ECs rescued the defective proliferation phenotype. Similar results were obtained when we analyzed the cell viability after serum starvation (Fig. 4c). ECs lacking Akt1 were more apoptotic after treatment with ceramide (as an apoptogen) using double staining (propidium iodide/ annexin V) analysis by flow cytometry (Fig. 4d) and cleaved caspase-3 expression analysis by Western blotting (Fig. 4e). In isolated aortic rings from Akt1$^{-/-}$mice, ceramide induced greater EC apoptosis (detected by TUNEL staining) as examined by *en face* imaging of EC (using PECAM-1 as a marker; Fig. 4f quantified in the right panel). Since EC apoptosis has been suggested as an initial step in atherogenesis, we studied EC apoptosis in the early stages of the lesion development in mice fed with a high cholesterol diet for only one month. As seen in Fig. 4g, there was a marked increase in apoptotic EC in aortic lesions from ApoE$^{-/-}$ Akt1$^{-/-}$ mice compared to littermate control mice.

Role of Akt1 on macrophage functions

Foam cell formation is a crucial step in atherogenesis (Glass and Witztum, 2001; Li and Glass, 2002). Circulating monocytes adhere to the activated endothelial cells and transmigrate into the intima to become tissue macrophages. Upon exposure to modified lipoproteins such as oxidized LDL, these macrophages differentiate into foam cells. To test whether Akt1 is important in monocyte adhesion, spreading and migration, we examined these processes in monocytes isolated from bone marrow. The adhesion, spreading and chemokine induced (MCP-1 and M-CSF) migration of monocytes was equivalent in cells isolated both groups of mice (Supplementary Fig. 2). Next, we investigated the binding and uptake of fluorescently labelled acetylated LDL (DiIacLDL). Flow cytometry analysis revealed no differences in the binding of lipoproteins (Fig. 5a) and a slight decrease in the uptake of DiI-acLDL (Fig. 5b). To examine cholesterol ester accumulation as an index of foam cell formation in vitro, peritoneal macrophages were isolated from ApoE$^{-/-}$ Akt1$^{-/-}$ and ApoE$^{-/-}$ mice and exposed to oxLDL *in vitro*. As shown in Fig. 5c, lipid accumulation in both groups was not significantly altered.

Akt1$^{-/-}$ macrophages are more susceptible to apoptosis

Death of foam cells by necrosis or apoptosis, particularly in the face of defective phagocytic clearance of the dead foam cells, is thought to give rise to large regions within plaques containing extra cellular lipid and necrotic debris (Li and Glass, 2002; Tabas, 2002). Interestingly, insulin receptor deficient macrophages promoted atherogenesis which correlated with lower levels of Akt phosphorylation (Han et al., 2006). To evaluate the role of Akt1 in macrophage survival, we incubated peritoneal macrophages in presence of oxLDL for 24 hours and the hypodiploid cells (necrotic and apoptotic cells) were analyzed by FACS. As seen in Fig. 5d ApoE$^{-/-}$ Akt1$^{-/-}$ cells were more susceptible to oxLDL induced apoptosis than control cells. In another set of experiments, to induce free cholesterol loading, macrophages were incubated with acLDL in presence of an ACAT inhibitor (58035) or oxLDL for 24 hours. Akt1$^{-/-}$ macrophages showed an increase in apoptosis under both conditions (Fig. 5e) indicating the important role of Akt1 in macrophage survival pathways. Increased numbers of TUNEL positive, CD68 positive macrophages were present in lesions from ApoE$^{-/-}$ Akt1$^{-/-}$ compared with ApoE $^{-/-}$ mice (Fig. 5f and quantified in right panel).

ApoE$^{-/-}$ bone marrow cells do not rescue atherosclerosis in the double mutant mice

To test whether an Akt1-dependent survival mechanism in macrophages accounts for the increase of atherosclerosis in the double mutant mice, bone marrow transplantation experiments were performed. Bone-marrow from ApoE$^{-/-}$ or ApoE$^{-/-}$ Akt1$^{-/-}$ was transplanted into 6-week-old, lethally irradiated ApoE$^{-/-}$ Akt1$^{-/-}$ or ApoE$^{-/-}$ mice, respectively. After four weeks of reconstitution, mice were fed with a high cholesterol diet for 12 weeks. ApoE$^{-/-}$ Akt1$^{-/-}$ bone-marrow cells transplanted into ApoE$^{-/-}$ mice were not sufficient to worsen lesion progression compared with ApoE$^{-/-}$ bone marrow transplanted into ApoE$^{-/-}$ Akt1$^{-/-}$ hosts (Fig. 5g *en face* and 5h for cross sections) demonstrating that the loss of Akt1 in bone marrow derived macrophages could not fully account for the enhanced aortic atherosclerosis in ApoE$^{-/-}$ Akt1$^{-/-}$ mice. These data suggest that vascular dysfunction in host mice lacking Akt1 is likely a major cause of lesion progression in ApoE$^{-/-}$Akt1$^{-/-}$ mice.

Absence of Akt1 increases the expression of inflammatory mediators and reduces eNOS phosphorilation in the vessel wall

Finally, to appreciate the multiple mechanisms of atherogenesis in intact vessels, we analyzed the quantitative expression patterns of markers of inflammation in the vessel wall of ApoE$^{-/-}$ Akt1$^{-/-}$ and ApoE$^{-/-}$ mice after 3 month on a high cholesterol diet by qPCR array technology. As seen in Fig. 6a, the expression levels of several inflammatory molecules were significantly upregulated in the double mutant mice compared to ApoE $^{-/-}$ alone such us interleukin-6 (IL-6), interleukin 13 receptor α 2 (IL-13ra2), tumor necrosis factor (Tnf). Vascular cell adhesion molecule 1 (VCAM-1) which is expressed after activation of endothelial cells and mediates the adhesion of leukocytes (Glass and Witztum, 2001) was also increased in ApoE $^{-/-}$ Akt1$^{-/-}$ aorta. Placental growth factor (Pgf) was increased while the angiogenesis inhibitor thrombospondin-1 (Thbs1) was decreased in the doubly mutant mice. To determine if the difference in pro-inflammatory gene expression was due to differences in intrinsic gene expression, cellularity or plaque composition in doubly mutant mice, we analyzed the expression of these genes in aortae from both groups of two months old mice fed a normal chow diet. As seen in Supplementary Fig. 3, no basal differences in gene expression were observed in both groups of mice.

We confirmed the increase of VCAM-1 expression in whole aorta by Western blotting (Fig. 6b and quantified in 6c). In addition, the levels of CD36, a member of the class B scavenger receptor family proteins involved in lipoprotein uptake (Calvo et al., 1998) and F4/80, a

membrane protein both expressed in monocytes/macrophages were highly expressed in both strains, but only F4/80 levels were statistically increased ApoE $^{-/-}$ Akt1$^{-/-}$ aortic lysates (Fig. 6b and 6c). The increase in inflammation and macrophages was associated with a marked reduction of eNOS phosphorylation on S1176 (but not total eNOS levels) consistent with less phosphorylation in both residues of Akt and with less total expression of Akt. The decrease in eNOS phosphorylation on S1176 was also seen on an additional Akt site (S617) using EC isolated from Akt1$^{-/-}$ mice; the reintroduction of Akt1 in Akt1$^{-/-}$ ECs rescued the defective phosphorylation phenotype (Supplementary Fig. 4).

Next, we analyzed the cellular localization of VCAM-1 in atherosclerotic lesions. As seen in Fig 7a, immunoreactive VCAM-1 is found in PECAM-1 positive EC but is also highly expressed in CD68 positive foam cells/macrophages in the atherosclerotic plaques. To test whether the increase in VCAM-1 expression correlated with more infiltration of macrophages into the lesion, we quantified VCAM-1 in CD68 positive cells. As shown in Fig. 7b, the macrophage infiltration (depicted by CD68 positive cells) was significantly higher in absence of Akt1. Moreover, the relative fluorescent intensity of VCAM-1 versus CD68 levels did not change indicating that the enhanced levels of VCAM-1 are due to increased macrophage infiltration in mice lacking Akt1 (Fig. 7c). To directly examine if the loss Akt1 influences VCAM-1 expression is EC, ICAM-1 and VCAM-1 surface levels were quantified by flow cytometry in EC isolated from WT and Akt1 $^{-/-}$ mice after stimulation with TNFα. As seen in Fig. 7d absence of Akt1 did not affect significantly the VCAM-1 and ICAM-1 expression in endothelial cells. Collectively, these data demonstrate that enhanced pro-inflammatory gene expression is secondary to macrophage infiltration in mice lacking Akt1 and the changing plaque composition triggered by EC dysfunction leads to an increased inflammatory plaque phenotype and larger lesions.

DISCUSSION

The major finding of this study is that a global absence of Akt1 in vivo enhances atherosclerotic lesion burden and promotes coronary atherosclerosis in a mouse model of atherosclerosis. Mechanistically, this phenotype is due to an increase in proatherogenic pathways such as enhanced apoptosis and less eNOS phosphorylation in ECs, and increased apoptosis in macrophages. Traditional hypotheses of atherogenesis have suggested that injury or dysfunction of vascular ECs is critical for the development of atherosclerosis (Littlewood and Bennett, 2003; Ross, 1990). The anatomical sites where atheromas develop are be associated with perturbed hemodynamics and increased EC turnover rate, suggesting a mechanical link with enhanced susceptibility to atherosclerosis, perhaps due to a decrease in NO bioavailability and an increase in EC apoptosis (Dimmeler et al., 1998). It has been reported that the regenerated ECs at sites of vascular damage do not function correctly (Fournet-Bourguignon et al., 2000); therefore, these dysfunctional cells will be unable to provide sufficient atheroprotection since they are deficient in NO bioactivity and other indices of endothelial dysfunction. In addition, enhanced susceptibility of the endothelium to local oxidative stress from LDL may change the apoptotic threshold in the absence of Akt1 and accelerate atherogenesis as observed in our model.

The relationship between macrophage apoptosis and atherogenesis is also complex (Tabas, 2005). Results from bone marrow transplantation studies using mice deficient in AIM (apoptosis inhibitor expressed by macrophages) or BAX, a proapoptotic protein, suggests that enhanced macrophage apoptosis in developing foam cells appears to limit lesion inflammation and progression (Arai et al., 2005; Liu et al., 2005). However, apoptotic macrophages are more abundant in advanced versus early atherosclerotic lesions, suggesting reduced or defective phagocytic clearance in advanced lesions (Tabas, 2002; Tabas, 2005). Consequently, this would result in postapoptotic macrophage necrosis and a heightened state

of inflammation in the vessel wall (Ball et al., 1995; Libby, 2002). In accordance with this, we found increased macrophage infiltration and increased proinflammatory gene expression (TNFα and IL-6) in vessels lacking Akt1. TNFα and IL-6 are amply expressed by foam cell macrophages (Li et al., 2005) and increased VCAM-1 and ICAM-1 expression on endothelial cells supports the further recruitment of monocytes into the atherosclerotic plaque (Tedgui and Mallat, 2006). Although VCAM-1 is inducibly expressed on EC, there is also marked expression of VCAM-1 on macrophages (Trogan et al., 2002), however its ligands and roles in atherogenesis are not known.

In contradistinction to the anti-atherosclerotic role of endogenous Akt in ApoE $^{-/-}$ Akt1$^{-/-}$ mice, the loss of Akt1 reduced LDL uptake by macrophages. This phenotype would favor atheroprotective mechanisms in the absence of Akt1 but clearly does not account for the role of Akt1 *in vivo*. Our data suggesting that Akt is atheroprotective via a vascular specific mechanism is supported by recent experiments showing that Akt1 is critical for endogenous NO production (Ackah et al., 2005) and vascular cell survival and transgenic expression of activated Akt in the endothelium, reduces vascular lesion formation in vivo (Mukai et al., 2006).

Murine models of atherosclerosis, such as apoE (apoE) or the LDL receptor knockout mice, usually do not exhibit many of the cardinal features of human coronary heart disease such as spontaneous myocardial infarction, atherothrombosis and premature death. Importantly, we describe here that the absence of Akt1 leads to extensive coronary atherosclerosis and increased mortality, unusual phenotypes previously observed in mice lacking at least two components of the cholesterol metabolic pathway (Braun et al., 2002; Caligiuri et al., 1999). Interestingly, peripheral coronary atherosclerosis was also observed in eNOS deficient mice bred to an atherosclerotic background (Kuhlencordt et al., 2001) which correlates with the reduce eNOS phosphorylation and activity that we observed in our model. Further studies are necessary to delineate the role of Akt1 in modifying plaque composition and to dissect the absolute importance of Akt1 in macrophages versus Akt1 in EC, however, bone marrow transplantation experiments favor a critical role of host Akt1 relative to macrophage Akt1 in this model. Collectively, these results suggest that the loss of Akt1 decreases EC NO production promoting EC activation which changes the apoptotic balance of vascular cells and macrophages thereby contributing to the progression of atherosclerosis. Thus, specific activation of Akt1 may provide a therapeutic approach to decrease atheroma formation and promote plaque stabilization while antagonizing Akt , an approach that may reduce tumor progression, may facilitate the progression of atherosclerosis. The increased atherogenesis in mice lacking Akt1 is mechanistically linked to endothelial cell dysfunction and enhanced macrophage dependent vascular inflammation.

EXPERIMENTAL PROCEDURES

Animal procedures

Akt1$^{-/-}$ mice were generated as previously described (Cho et al., 2001b). Akt1$^{-/-}$ mice that have been backcrossed 8 generations onto a C57BL/6 background were crossed with ApoE-deficient mice, also on the C57BL/6 background, to generate mice heterozygous at both loci. These ApoE+/− Akt1+/− mice were crossed a second time with ApoE$^{-/-}$ mice. The ApoE$^{-/-}$ Akt1$^{-/+}$ progeny from this round of breeding were then intercrossed to produce ApoE$^{-/-}$ Akt1$^{-/-}$ and ApoE$^{-/-}$ Akt1$^{+/+}$ littermates that were used as controls for all studies. Accelerated atherosclerosis was induced by feeding the mice for 14 weeks with a high cholesterol diet containing 1.25% cholesterol (ResearchDiets, D12108). All the experiments were approved by the Institutional Animal Care Use Committee of Yale University.

Lipids analysis and lipoprotein profiles measurement

Mice were fasted for 12–14h before blood samples were collected by retro-orbital venous plexus puncture. Plasma was separated by centrifugation and stored at −80°C. Total plasma cholesterol and triglycerides were enzymatically measured using the Amplex red cholesterol assay kit (Molecular Probes) and serum triglyceride determination kit (Sigma) respectively according to the manufacture's instructions. The lipid distribution in plasma lipoprotein fractions were assessed by fast-performance liquid chromatography (FPLC) gel filtration with 2 Superose 6 HR 10/30 columns (Pharmacia).

Bone marrow transplantation

Eight-week-old male or female ApoE$^{-/-}$ or Akt1$^{-/+}$ApoE$^{-/-}$ were lethally irradiated with 1000 rads (10Gy) from a cesium source 4 hours before transplantation. Bone marrow were collected from femurs of donor ApoE$^{-/-}$ or ApoE$^{-/-}$ Akt1$^{-/-}$ mice by flushing with sterile medium (RPMI 1640), 2% FBS, 5U/ml heparin, 50U/ml penicillin, 50μg/ml streptomycin). Each recipient mouse was injected with 2×10^6 bone marrow cells through the jugular vein. Four weeks after bone marrow (BM) transplantation, peripheral blood was collected retro-orbital venous plexus puncture for PCR analysis of bone marrow reconstitution. For atherosclerosis study, the mice were fed with high cholesterol diet for 10 weeks beginning 4 weeks after BM transplantation and based on PCR genotyping were fully chimeric.

Atherosclerotic lesion analysis

After 12 weeks of being fed a Western-type diet, mice were anesthetized and euthanized. Mouse hearts were perfused using 10 ml of PBS (Invitrogen) followed by 10 ml of 4% Para-formaldehyde (PFA). After incubation in 4% PFA overnight, the adventitia was thoroughly cleaned under a dissecting microscope, and the aorta was cut open longitudinally and pinned on to a silicone plate. To calculate the lesion area, aortas were stained with Oil Red O (Sigma) before the analysis. Oil Red stock solution (35ml; 0.2% weight/volume in methanol) was mixed with 10 ml of 1 M NaOH and filtered. Aortas were briefly rinsed with 78% methanol, incubated in Oil Red O solution for 50 min, then destained in 78% methanol for 5 min and mounted on microscopic slides using aqueous mounting medium (Stephens Scientific). Plaques were analyzed under the Nikon SMZ 1000 microscope, connected to a Kodak DC290 digital camera. The images were analyzed using Adobe Photoshop 6.0 (Adobe) and the lesions quantified using the IMAGE J (NIH) program. For other images, 10-μm thick cryosections of the proximal aorta were serially sectioned and stained with hematoxylin/eosin for quantifications of the lesion areas using IMAGE J (NIH) program. Aortic lesion size of each animal was obtained by averaging lesion areas in six sections from the same mouse.

Angiography

After 12 weeks on high cholesterol diet, mice were anesthetized and heparinzed. The hearts ascending aorta was perfused with PBS containing the vasodilators (papaverine, 4 mg/liter; adenosine, 1 g/liter) for 3 min at physiological pressure through descending aorta, and blood was drained from the right atrium. The vasculature were fixed with 2% paraformaldehyde (in PBS) for 5 min, flushed with PBS for 2 min, and infused with contrast agent (bismuth oxychloride in saline and 10% gelatin in PBS 1:1). Mice were then immersed in ice to solidify the contrast agent. Microangiography was taken with Faxitron x-ray machine (Hewlett-Packard) at 25 kV for 15 sec.

MLEC isolation

MLEC were isolated from 3-week-old Akt1$^{-/-}$ and WT mice. Briefly, mice were euthanized with an overdose of ketamine/xylazine and the lungs were excised, minced and digested

with 0.1% collagenase in RPMI medium. The digest was homogenized by passing multiple times through a 14-gauge needle. It was then filtered through a 150-μm tissue sieve, and the cell suspension was plated on 0,1 gelatin-coated dishes. After 2 to 3, cells, cells were immortalized by 2 rounds of infection with retrovirus encoding the middle T antigen. Cells were allowed to recover for 24 hours, and then ECs were isolated by immunoselection with PECAM-1 and ICAM-2- conjugated magnetic beads. When cells reached confluency, a second round of immunoselection was performed. Cells were propagated in EGM-2 media supplemented with EGM-2 microvascular (MV) SingleQuots (Cambrex). For $Akt1^{-/-}$ reconstitution, cells were infected twice with a retrovirus encoding either HA-tagged murine Akt1 or GFP

Cell migration assay

Cell migraton assays were performed using a modified Boyden chamber with Costar Transwell inserts (Corning). The inserts were coated with a solution of 0.1% gelatin. Subconfluent monocyte were serum starved overnight. Solutions of MCP-1 (100 ng/ml), M-CSF (100 ng/ml) and 10% FBS were prepared in DMEM and added to the bottom chambers. Monocytes (7.5×10^4 cells) were added to the upper chambers. After 6 hours incubation at 37°C, cells on both sides of the membrane were fixed and stained with the Diff-Quik staining kit (Baxter Health). Cells on the upper side of the membrane were removed with a cotton swab. The average number of cells per field on the lower side of the membrane from 4 high-power (x400) fields was counted.

Cell proliferation assay

Cell number and viability was determined by Tripan blue dye exclusion using a hemocytometer.

Foam cell formation

Thioglycolate-elicited peritoneal macrophages were plated on 12-well plates in RPMI 1640 supplemented with 10% FBS, 100 units/ml penicillin and 100 μg/ml streptomycin. After 2 hours, non-adherent cells were washed out and macrophages were incubated in fresh medium for 24 hours. Then, oxLDL (100 μg/ml) (Intracel Inc) was added to the medium. After about 24 hours cells were stained for 60 min with Oil Red O.

Binding and uptake of acLDL

Thioglycolate-elicited peritoneal macrophage were plated on 6 cm dishes in RPMI 1640 supplemented with 10% FBS, 100 units/ml penicillin and 100 μg/ml streptomycin. After 2 hours, non-adherent cells were washed out and macrophages were incubated in RPMI 1640 medium supplemented with 10% lipoprotein deficient media (LPDS) for 24 hours. For binding studies, adherent cells were incubated with 10 μg/ml DiI-acLDL for 2h at 4°C. To analyze the uptake of DiI-acLDL, cells were incubated for 2h at 37°C. In order to exclude non-specific binding and uptake, we supplemented the medium with an excess of unlabeled acLDL (200 μg/ml). Finally, the samples were washed, resuspended in 1 ml of PBS and analyzed by flow cytometry (FACSort, Becton Dickinson). The results are expressed in terms of specific median intensity of fluorescence (M.I.F.) after subtracting the M.I.F. of cells incubated in excess of unlabelled acLDL.

Western blot analysis

Tissues were snap frozen in liquid nitrogen, pulverized, and resuspended in lysis buffer: 50 mM Tris-HCl, pH 7.4, 0.1 mM EDTA, 0.1 mM EGTA, 1% NP-40, 0,1% sodium deoxycholate, 0,1% SDS, 100 mM NaCl, 10 mM NaF, 1 mM sodium pyrophosphate, 1 mM sodium orthovanadate, 1 mM Pefabloc SC, and 2 mg/ml protease inhibitor cocktail (Roche

Diagnostics Corp). Cells were lysed on ice with lysis buffer as noted above. Protein concentrations were determined using the DC Protein assay kit (Bio-Rad Laboratories). Lysates containing 80 μg (tissue) or 30 μg (cells) of protein were analyzed by SDS-PAGE and immunoblotting. Primary antibodies used include the following: Akt1 m-Ab (Upstate), Akt p-Ab, p-Akt473 p-Ab, p-Akt308 m-Ab, cleaved caspase3 p-Ab, caspase3 (Cell signaling), eNOS m-Ab, heat shock protein (Hsp90) m-Ab (BD Transduction Laboratories; BD Biosciences-Pharmingen), CD36 p-Ab, VCAM-1 p-Ab (Santa Cruz) and F4/80 (Serotec). Secondary antibodies were fluorescence-labeled antibodies (LI-COR Biotechnology). Bands were visualized using the Odyssey Infrared Imaging System (LI-COR Biotechnology).

Flow cytometry analysis

Apoptotic cells were determined by their hypochromic, subdiploid staining profiles (SubG1 population). Serum-starved ECs or peritoneal macrophages cultured in presence of 100 μg/ml oxLDL, were stained with propidium iodide (PI) and analyzed by flow cytometry (FACSort, Becton Dickinson). For staining, one million cells were harvested, washed in PBS and then fixed with 70 % ethanol. Fixed cells were treated with DNAsefree RNAse (Roche) for 30 min at 37°C, washed in PBS, centrifuged, and incubated in PBS containing PI (25 μg/ml; Sigma). Forward light scatter characteristics were used to exclude cell debris from the analysis. To estimate early apoptosis cells, Alexa FITC-conjugated annexin V (Molecular Probes, Inc) was used together with PI dead cell counterstain following the manufacturer´s recommendations.

Macrophage apoptosis assays

Peritoneal macrophages from WT and Akt1$^{-/-}$ mice fed regular chow diet were harvested with PBS 3 days after intraperitoneal injection of thioglycolate. The macrophages were plated on 12-well plates in RPMI 1640 supplemented with 10% FBS, 100 units/ml penicillin and 100 μg/ml streptomycin. After 2 hours, non-adherent cells were washed out and macrophages were incubated in fresh medium for 24 hours. Then, cells were incubated with 100 μg/ml acLDL (Intracel, Inc) and 10 μg/ml 58035, an ACAT inhibitor (Sigma) or with 100 μg/ml oxLDL (Intracel, Inc) for about 24 hours. Apoptosis assays were performed by staining macrophages with Alexa 488-labeled annexin V, using Vybrant Apoptosis Assay Kit (Molecular Probes) or analyzing the subdiploid staining profiles (SubG1 population) as described above.

Immunohistochemistry

Snap-frozen fixed aortic rings embedded in OCT were sectioned, fixed in acetone and processed for antibody staining according to standard protocols. The following antibodies were used: anti PECAM-1 (BD Bioscience) and CD68 (Serotec). Positive cells and total cells were quantified of the aortic arch (five different sections) from four different mice of each genotyping using IMAGE J software. Whole-mount immunostaining was performed as previously described(Murata et al., 2002). After the fixation, arteries were probed with anti-PECAM antibody (1:200) for 12h at 4°C. For the detection of apoptosis, fluorescein isothiocyanate (FITC)-labeled dUTP nick endlabeling (TUNEL) method was applied to the sections using an In Situ Apoptosis Detection Kit-POD following the instruction (Roche Diagnostics, USA).

Gene Expression Analysis by PCR Array

RT^2 *Profiler*™ PCR Array from SuperArray Bioscience Corporation was used to examine the expression pattern of genes involved in atherosclerosis. Each array consists of 84 key genes involved in modulating atherosclerosis, angiogenesis and inflammation as well as 5

housekeeping (HK) genes used for normalizing the PCR Array data. Using different arrays, we compared the aortic gene expression of mice before and after 3 months of diet. For these experiments, a combined TRizol/Qiagen protocol was used to extract RNA. Briefly, aortas were isolated, frozen, crushed and resuspended in 1 ml TRIzol. The RNA-containing phase was recovered after spinning for 10 min at 10,000 × g, mixed with an equal volume of 70% ethanol and applied on a Qiagen RNeasy column. The remaining steps were carried out according to Qiagen's protocols. cDNA was prepared as above from 2 μg of total RNA. Then the Real-Time PCR Array was performed as indicated in the user manual using the specific RT^2 Real-Time™ SYBR Green/Fluorescein (SuperArray Bioscience Corporation). Three independent arrays were carried out for each condition using iCycler (BioRad). The fold-change for each gene from mice after diet to before diet was calculated as $2^{(-\Delta\Delta C)}{}_t$, where $\Delta\Delta C_t = \Delta C_t$ after diet - ΔC_t siRNA before diet and where $\Delta C_t = C_{t\ \text{gene of interest}} - C_{t\ \text{average of HK genes}}$ for each treatment.

Statistical analysis

Data are presented as mean ± SEM (n is noted in the fig legends) and statistical significance of differences was evaluated with student´s t test. Significance was accepted at the level of $p<0.05$.

Supplementary Material

Refer to Web version on PubMed Central for supplementary material.

Acknowledgments

The authors would like to thank Dr. Themis Kyriakides for help with bone marrow experiments and monocyte isolation. This work was supported by grants R01 HL64793, R01 HL61371, R01 HL57665 and P01 Hl70295 from the National Institutes of Health to W.C. Sessa, a Fellowship from Ministerio de Educación y Ciencia, Spain and Philip Morris External Research Postdoctoral Fellowship, USA (to C. Fernández-Hernando), a Medical Scientist Training Program grant GM07205 (to E. Ackah) and a Programme 3+3 Fellowship from the Centro Nacional de Investigaciones Cardiovasculares (CNIC) (to Y. Suárez).

REFERENCES

Ackah E, Yu J, Zoellner S, Iwakiri Y, Skurk C, Shibata R, Ouchi N, Easton RM, Galasso G, Birnbaum MJ, et al. Akt1/protein kinase Balpha is critical for ischemic and VEGF-mediated angiogenesis. J Clin Invest. 2005; 115:2119–2127. [PubMed: 16075056]

Arai S, Shelton JM, Chen M, Bradley MN, Castrillo A, Bookout AL, Mak PA, Edwards PA, Mangelsdorf DJ, Tontonoz P, Miyazaki T. A role for the apoptosis inhibitory factor AIM/Spalpha/Api6 in atherosclerosis development. Cell Metab. 2005; 1:201–213. [PubMed: 16054063]

Ball RY, Stowers EC, Burton JH, Cary NR, Skepper JN, Mitchinson MJ. Evidence that the death of macrophage foam cells contributes to the lipid core of atheroma. Atherosclerosis. 1995; 114:45–54. [PubMed: 7605375]

Braun A, Trigatti BL, Post MJ, Sato K, Simons M, Edelberg JM, Rosenberg RD, Schrenzel M, Krieger M. Loss of SR-BI expression leads to the early onset of occlusive atherosclerotic coronary artery disease, spontaneous myocardial infarctions, severe cardiac dysfunction, and premature death in apolipoprotein Edeficient mice. Circ Res. 2002; 90:270–276. [PubMed: 11861414]

Caligiuri G, Levy B, Pernow J, Thoren P, Hansson GK. Myocardial infarction mediated by endothelin receptor signaling in hypercholesterolemic mice. Proc Natl Acad Sci U S A. 1999; 96:6920–6924. [PubMed: 10359814]

Calvo D, Gomez-Coronado D, Suarez Y, Lasuncion MA, Vega MA. Human CD36 is a high affinity receptor for the native lipoproteins HDL, LDL, and VLDL. J Lipid Res. 1998; 39:777–788. [PubMed: 9555943]

Cantley LC. The phosphoinositide 3-kinase pathway. Science. 2002; 296:1655–1657. [PubMed: 12040186]

Chen J, Somanath PR, Razorenova O, Chen WS, Hay N, Bornstein P, Byzova TV. Akt1 regulates pathological angiogenesis, vascular maturation and permeability in vivo. Nat Med. 2005; 11:1188–1196. [PubMed: 16227992]

Chen WS, Xu PZ, Gottlob K, Chen ML, Sokol K, Shiyanova T, Roninson I, Weng W, Suzuki R, Tobe K, et al. Growth retardation and increased apoptosis in mice with homozygous disruption of the Akt1 gene. Genes Dev. 2001; 15:2203–2208. [PubMed: 11544177]

Cho H, Mu J, Kim JK, Thorvaldsen JL, Chu Q, Crenshaw EB 3rd, Kaestner KH, Bartolomei MS, Shulman GI, Birnbaum MJ. Insulin resistance and a diabetes mellitus-like syndrome in mice lacking the protein kinase Akt2 (PKB beta). Science. 2001a; 292:1728–1731. [PubMed: 11387480]

Cho H, Thorvaldsen JL, Chu Q, Feng F, Birnbaum MJ. Akt1/PKBalpha is required for normal growth but dispensable for maintenance of glucose homeostasis in mice. J Biol Chem. 2001b; 276:38349–38352. [PubMed: 11533044]

Cozen AE, Moriwaki H, Kremen M, DeYoung MB, Dichek HL, Slezicki KI, Young SG, Veniant M, Dichek DA. Macrophage-targeted overexpression of urokinase causes accelerated atherosclerosis, coronary artery occlusions, and premature death. Circulation. 2004; 109:2129–2135. [PubMed: 15096455]

Dimmeler S, Hermann C, Zeiher AM. Apoptosis of endothelial cells. Contribution to the pathophysiology of atherosclerosis? Eur Cytokine Netw. 1998; 9:697–698. [PubMed: 9889419]

Dzau VJ, Braun-Dullaeus RC, Sedding DG. Vascular proliferation and atherosclerosis: new perspectives and therapeutic strategies. Nat Med. 2002; 8:1249–1256. [PubMed: 12411952]

Easton RM, Cho H, Roovers K, Shineman DW, Mizrahi M, Forman MS, Lee VM, Szabolcs M, de Jong R, Oltersdorf T, et al. Role for Akt3/protein kinase Bgamma in attainment of normal brain size. Mol Cell Biol. 2005; 25:1869–1878. [PubMed: 15713641]

Fournet-Bourguignon MP, Castedo-Delrieu M, Bidouard JP, Leonce S, Saboureau D, Delescluse I, Vilaine JP, Vanhoutte PM. Phenotypic and functional changes in regenerated porcine coronary endothelial cells : increased uptake of modified LDL and reduced production of NO. Circ Res. 2000; 86:854–861. [PubMed: 10785507]

Glass CK, Witztum JL. Atherosclerosis. the road ahead. Cell. 2001; 104:503–516. [PubMed: 11239408]

Han S, Liang CP, DeVries-Seimon T, Ranalletta M, Welch CL, Collins- Fletcher K, Accili D, Tabas I, Tall AR. Macrophage insulin receptor deficiency increases ER stress-induced apoptosis and necrotic core formation in advanced atherosclerotic lesions. Cell Metab. 2006; 3:257–266. [PubMed: 16581003]

Ignarro LJ, Napoli C. Novel features of nitric oxide, endothelial nitric oxide synthase, and atherosclerosis. Curr Atheroscler Rep. 2004; 6:281–287. [PubMed: 15191702]

Kuhlencordt PJ, Gyurko R, Han F, Scherrer-Crosbie M, Aretz TH, Hajjar R, Picard MH, Huang PL. Accelerated atherosclerosis, aortic aneurysm formation, and ischemic heart disease in apolipoprotein E/endothelial nitric oxide synthase double-knockout mice. Circulation. 2001; 104:448–454. [PubMed: 11468208]

Li AC, Glass CK. The macrophage foam cell as a target for therapeutic intervention. Nat Med. 2002; 8:1235–1242. [PubMed: 12411950]

Li Y, Schwabe RF, DeVries-Seimon T, Yao PM, Gerbod-Giannone MC, Tall AR, Davis RJ, Flavell R, Brenner DA, Tabas I. Free cholesterolloaded macrophages are an abundant source of tumor necrosis factor-alpha and interleukin-6: model of NF-kappaB- and map kinase-dependent inflammation in advanced atherosclerosis. J Biol Chem. 2005; 280:21763–21772. [PubMed: 15826936]

Libby P. Inflammation in atherosclerosis. Nature. 2002; 420:868–874. [PubMed: 12490960]

Littlewood TD, Bennett MR. Apoptotic cell death in atherosclerosis. Curr Opin Lipidol. 2003; 14:469–475. [PubMed: 14501585]

Liu J, Thewke DP, Su YR, Linton MF, Fazio S, Sinensky MS. Reduced macrophage apoptosis is associated with accelerated atherosclerosis in lowdensity lipoprotein receptor-null mice. Arterioscler Thromb Vasc Biol. 2005; 25:174–179. [PubMed: 15499039]

Mukai Y, Rikitake Y, Shiojima I, Wolfrum S, Satoh M, Takeshita K, Hiroi Y, Salomone S, Kim HH, Benjamin LE, et al. Decreased vascular lesion formation in mice with inducible endothelial-specific expression of protein kinase Akt. J Clin Invest. 2006; 116:334–343. [PubMed: 16453020]

Murata T, Sato K, Hori M, Ozaki H, Karaki H. Decreased endothelial nitric-oxide synthase (eNOS) activity resulting from abnormal interaction between eNOS and its regulatory proteins in hypoxia-induced pulmonary hypertension. J Biol Chem. 2002; 277:44085–44092. [PubMed: 12185080]

Nakashima Y, Plump AS, Raines EW, Breslow JL, Ross R. ApoEdeficient mice develop lesions of all phases of atherosclerosis throughout the arterial tree. Arterioscler Thromb. 1994; 14:133–140. [PubMed: 8274468]

Phung TL, Ziv K, Dabydeen D, Eyiah-Mensah G, Riveros M, Perruzzi C, Sun J, Monahan-Earley RA, Shiojima I, Nagy JA, et al. Pathological angiogenesis is induced by sustained Akt signaling and inhibited by rapamycin. Cancer Cell. 2006; 10:159–170. [PubMed: 16904613]

Reddick RL, Zhang SH, Maeda N. Atherosclerosis in mice lacking apo E. Evaluation of lesional development and progression. Arterioscler Thromb. 1994; 14:141–147. [PubMed: 8274470]

Ross R. Mechanisms of atherosclerosis--a review. Adv Nephrol Necker Hosp. 1990; 19:79–86. [PubMed: 2105588]

Shiojima I, Sato K, Izumiya Y, Schiekofer S, Ito M, Liao R, Colucci WS, Walsh K. Disruption of coordinated cardiac hypertrophy and angiogenesis contributes to the transition to heart failure. J Clin Invest. 2005; 115:2108–2118. [PubMed: 16075055]

Tabas I. Consequences of cellular cholesterol accumulation: basic concepts and physiological implications. J Clin Invest. 2002; 110:905–911. [PubMed: 12370266]

Tabas I. Consequences and therapeutic implications of macrophage apoptosis in atherosclerosis: the importance of lesion stage and phagocytic efficiency. Arterioscler Thromb Vasc Biol. 2005; 25:2255–2264. [PubMed: 16141399]

Tedgui A, Mallat Z. Cytokines in atherosclerosis: pathogenic and regulatory pathways. Physiol Rev. 2006; 86:515–581. [PubMed: 16601268]

Tricot O, Mallat Z, Heymes C, Belmin J, Leseche G, Tedgui A. Relation between endothelial cell apoptosis and blood flow direction in human atherosclerotic plaques. Circulation. 2000; 101:2450–2453. [PubMed: 10831515]

Trogan E, Choudhury RP, Dansky HM, Rong JX, Breslow JL, Fisher EA. Laser capture microdissection analysis of gene expression in macrophages from atherosclerotic lesions of apolipoprotein E-deficient mice. Proc Natl Acad Sci U S A. 2002; 99:2234–2239. [PubMed: 11842210]

Tschopp O, Yang ZZ, Brodbeck D, Dummler BA, Hemmings-Mieszczak M, Watanabe T, Michaelis T, Frahm J, Hemmings BA. Essential role of protein kinase B gamma (PKB gamma/Akt3) in postnatal brain development but not in glucose homeostasis. Development. 2005; 132:2943–2954. [PubMed: 15930105]

Whiteman EL, Cho H, Birnbaum MJ. Role of Akt/protein kinase B in metabolism. Trends Endocrinol Metab. 2002; 13:444–451. [PubMed: 12431841]

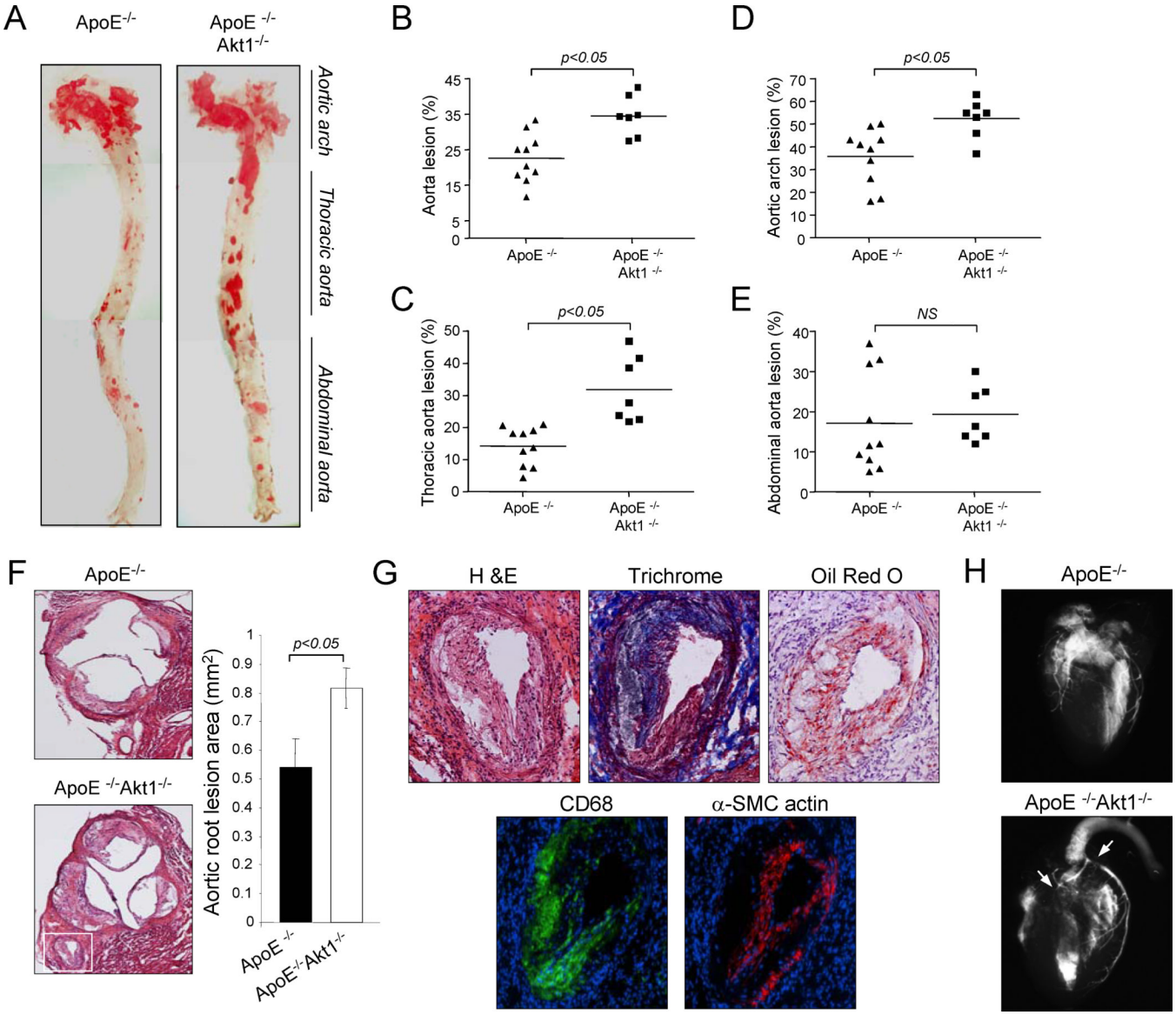

Fig. 1. Deletion of Akt1 accelerates atherosclerosis in ApoE$^{-/-}$ mice

(a-e). Oil-Red O staining of aortas from mice with the indicated genotypes. Atheroma formation was significantly increased in ApoE$^{-/-}$Akt1$^{-/-}$ mice (n=7 mice), compared to ApoE$^{-/-}$ littermates (n=10). **(f)** Representative examples of cross sections from the aortic sinus stained with hematoxylin/eosin. Inset refers to lesions in the coronary ostia of Akt1$^{-/-}$ ApoE$^{-/-}$ mice. Quantification of atheroma area. All of the data represent the mean ± S.E.M; n=5 mice in each group). **(g)** Representative histological analysis of coronary arteries stained with hematoxylin/eosin, trichrome, Oil red O, CD68 (a macrophage marker) and α-smooth muscle cell actin. **(h)** Ex vivo angiograms of ApoE$^{-/-}$ (top) and ApoE$^{-/-}$Akt1$^{-/-}$ (botton) hearts. Arrowheads indicate multiple severe stenoses in coronary arteries.

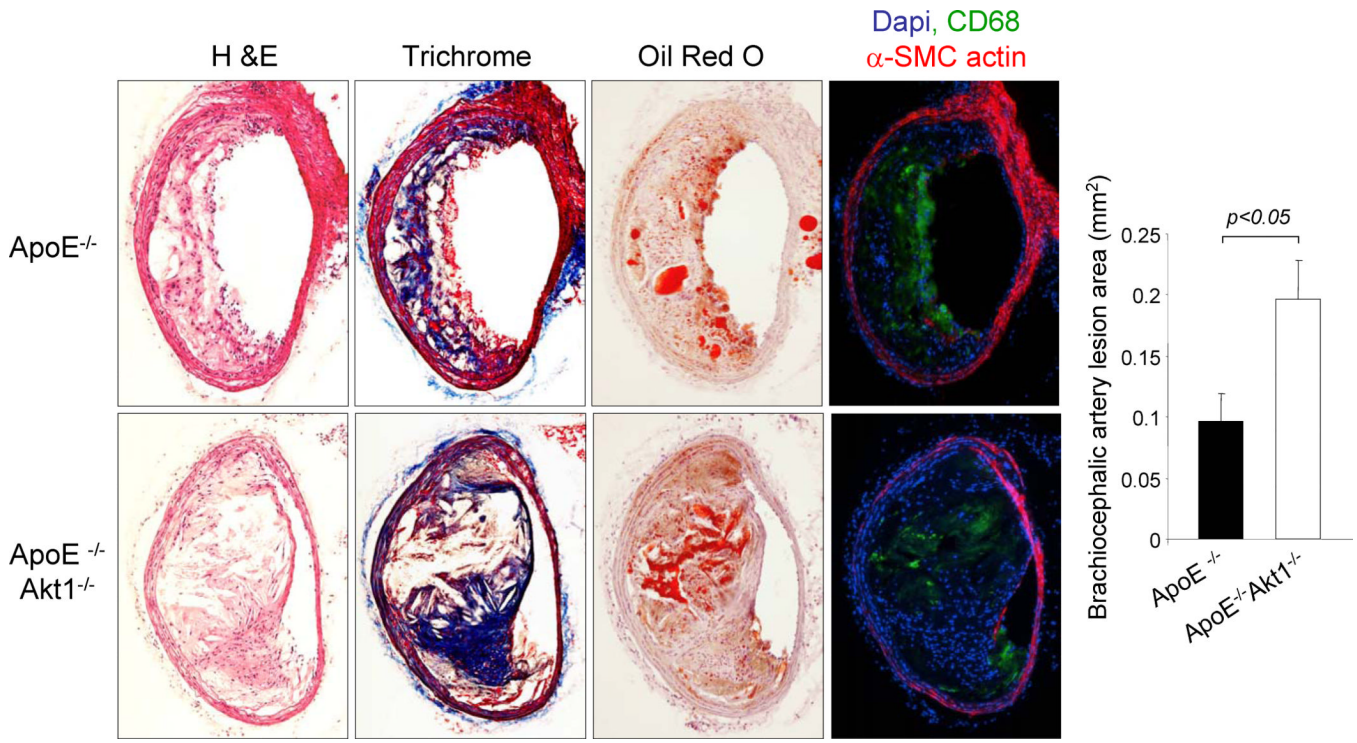

Fig. 2. The absence of Akt1 increases lesion expansion in the innominate/brachiocephalic trunk in ApoE$^{-/-}$ mice

Representative histological analysis of cross sections from the brachiocephalic arteries stained with hematoxylin/eosin, trichrome, Oil red O, CD68 (a macrophage marker) and α-smooth muscle cell actin. Quantification of atheroma area (right panel). All of the data represent the mean ± S.E.M; n=5 mice (males) in each group.

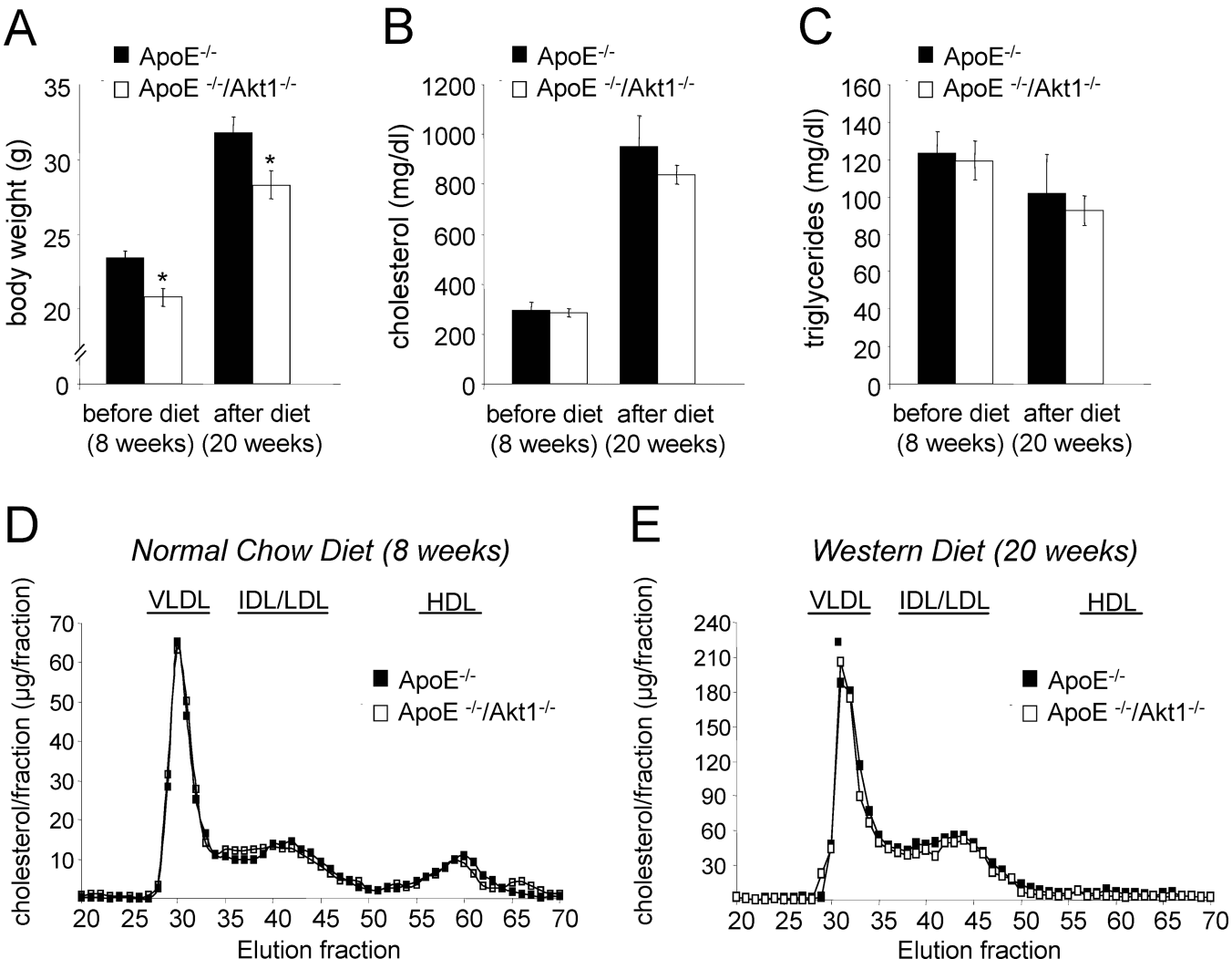

Fig. 3. Reduced body weight in absence of Akt1 and similar values of cholesterol, triglycerides and lipoprotein profiles

(a) Body weight of Akt1+/+ApoE$^{-/-}$ (n=10) and Akt1$^{-/-}$ ApoE$^{-/-}$ (n=8) mice before and after 12 weeks on high cholesterol diet. *, $p < 0.05$ compared with Akt1$^{+/+}$ApoE$^{-/-}$. **(b)** Fasting cholesterol levels of ApoE$^{-/-}$ and Akt1$^{-/-}$ ApoE$^{-/-}$ mice before and after 12 weeks on high cholesterol diet. **(c)** Fasting triglycerides levels from both groups of mice before and after 12 weeks on high cholesterol diet. **(d)**Lipoprotein profiles from ApoE$^{-/-}$ and double mutant mice before and after diet.

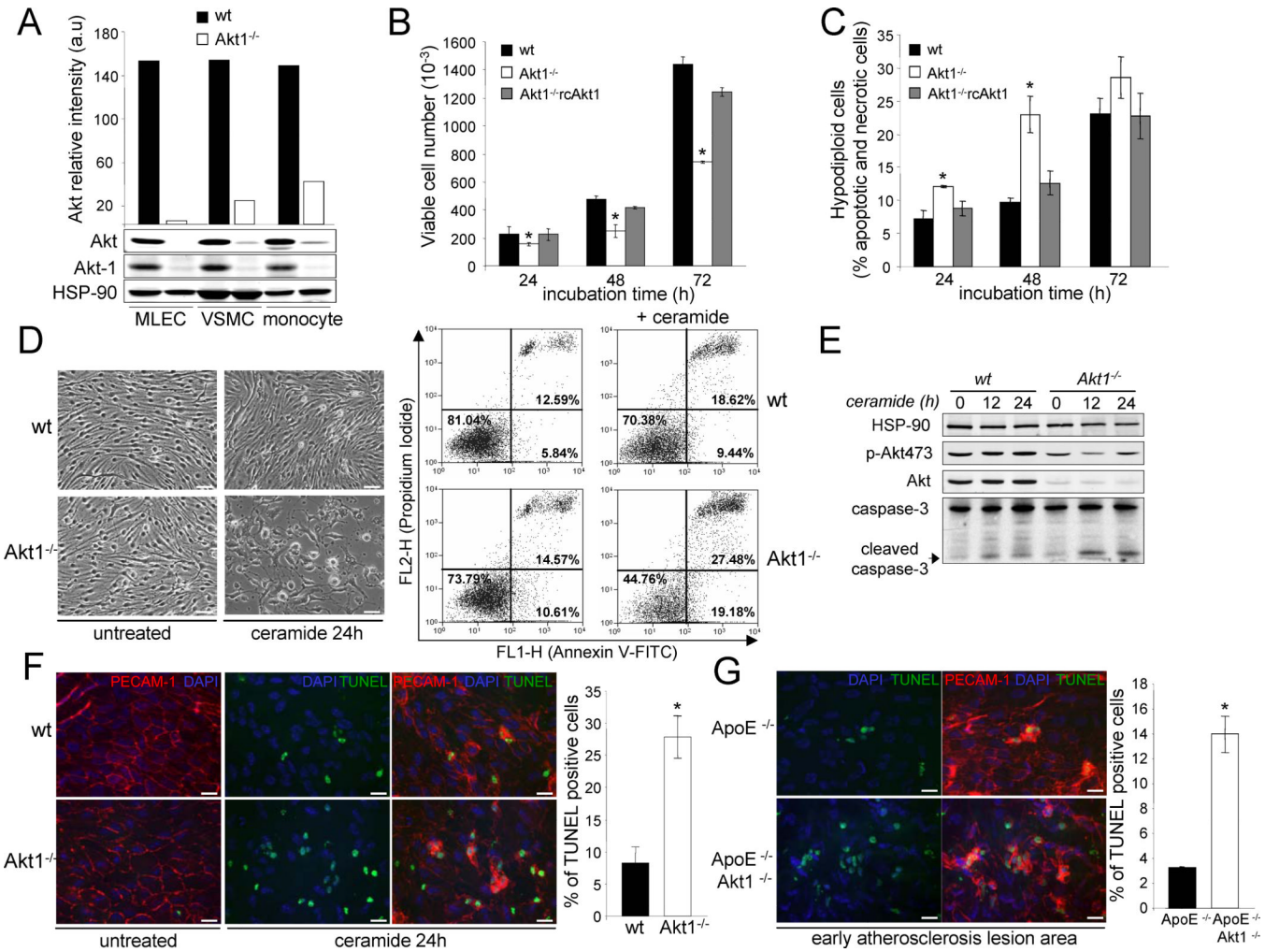

Fig. 4. Absence of Akt1, the predominant isoform in EC, VSMC and monocytes reduces endothelial cell proliferation and viability in vitro and in vivo

(a) Western blot analysis and densitometry of total Akt protein expression levels in lung ECs, aortic VSMC and bone marrow derived monocytes. **(b,c)** EC proliferation (b) measured as viable cell number and apoptotic cells (c) determined by their hypochromic, subdiploid staining profiles (SubG1 population) after incubation the wild type and Akt1$^{-/-}$ ECs in absence of serum at different time points. The data represent the mean ± S.E.M. of triplicate samples repeated in three separate experiments.*, $p < 0.05$ compared with wild type cells. **(d)** Phase-contrast micrographs of cultures treated or not for 24 h with ceramide (30 μM) and dot-plot diagrams of FITC-conjugated annexin V and PI. Results are representative of two separate experiments which gave similar results. **(e)** Western blot analyses of cleaved caspase-3, Akt and phopho-Akt473 from wild type and Akt1$^{-/-}$ ECs treated with ceramide (30 μM) for 12 and 24 h. The Western blots are representative of two separate experiments which gave similar results. **(f)** Whole-mount en face immunostaining of WT and Akt1$^{-/-}$ aortas treated with ceramide (30 μM) for 24 Apoptotic cells were detected by TUNEL staining and EC by PECAM-1 staining. Representative fluorescent images (20X magnification) and quantitative data are shown to the right. The data are expressed as the percentage of TUNEL-positive cells per field (4 fields per three mice each group). Bars, 25μm. **(g)** Apoptotic cells in the lesion area from ApoE$^{-/-}$ and ApoE$^{-/-}$ Akt1$^{-/-}$ after 4 weeks of high cholesterol diet were detected by TUNEL staining.

Representative fluorescence images are shown and quantitative data are shown to the right. Bars, 25μm.

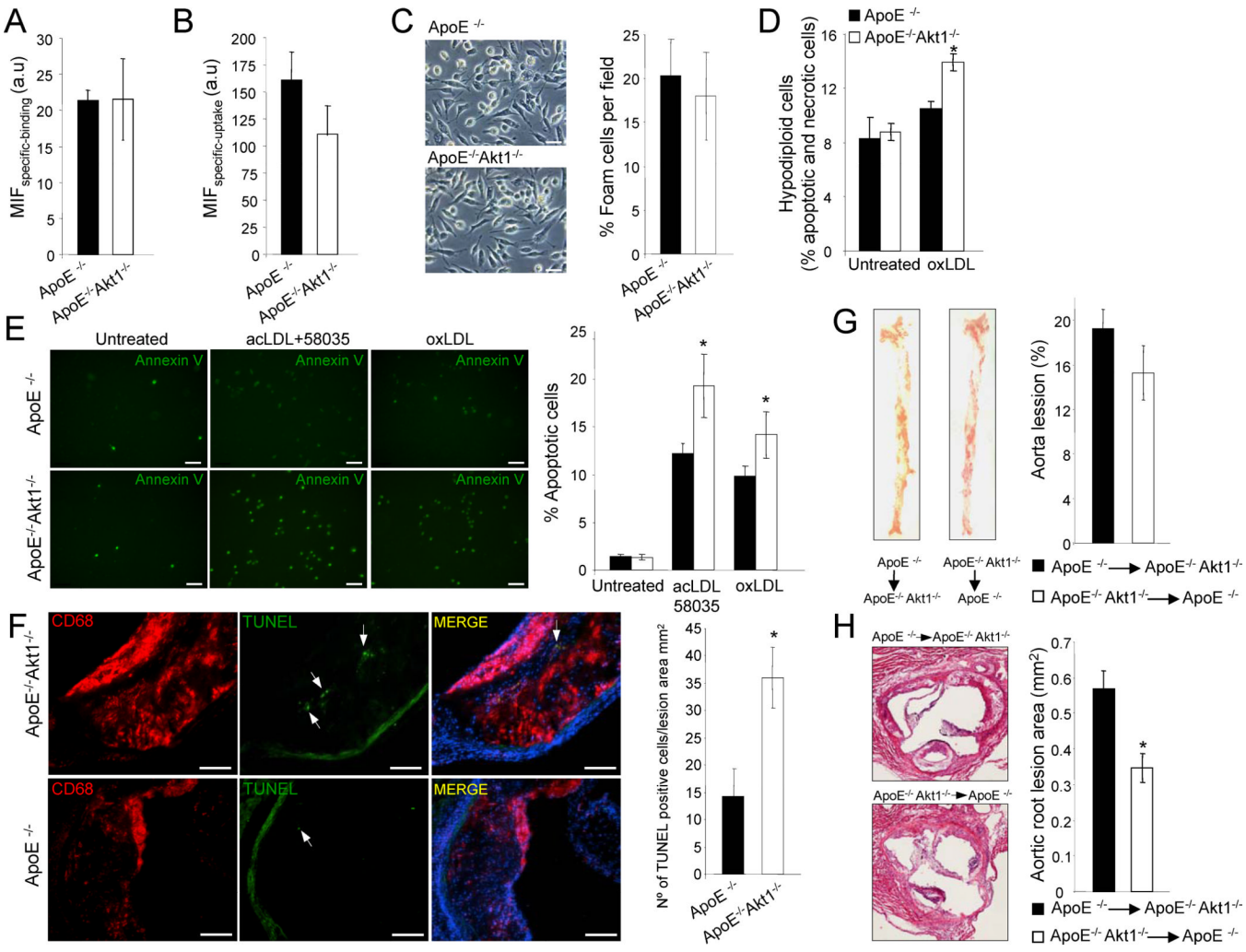

Fig. 5. Akt1$^{-/-}$ macrophages display similar binding to lipoproteins and foam cell formation and shown increased susceptibility to apoptosis by cholesterol overload

Specific binding **(a)** and uptake **(b)** of DiI-labeled acLDL in peritoneal macrophages isolated from ApoE$^{-/-}$ and ApoE$^{-/-}$ Akt1$^{-/-}$ mice. The data are mean ± S.E. of triplicate samples repeated in two separate experiments. **(c)** Foam cells from ApoE$^{-/-}$ and ApoE$^{-/-}$ Akt1$^{-/-}$ mice treated with oxLDL for 24h and quantitative analysis of three independent experiments. Bars, 50μm. **(d)** Apoptotic cells determined by their hypochromic, subdiploid staining profiles (SubG1 population) after incubation ApoE$^{-/-}$ and ApoE$^{-/-}$ Akt1$^{-/-}$ peritoneal macrophage with (oxLDL100 μg/ml) for 24h. The data are mean ± S.E.M. of triplicate samples repeated from three different groups of mice.*, $p < 0.05$ compared with ApoE$^{-/-}$. **(e)** Quantitative determination of apoptotic macrophages stained positive for annexin V. Thioglicollate-elicited peritoneal macrophage from either ApoE$^{-/-}$ and ApoE$^{-/-}$ Akt1$^{-/-}$ mice were incubated with or without acLDL (100 μg/ml) and 58035, (10 μg/ml) an ACAT inhibitor or oxLDL (100 μg/ml) for 36h. All results represent mean ± S.E.M. of triplicate samples from three different sets of mice. Bars, 100μm. **(f)** Apoptotic cells and macrophages in lesions from ApoE$^{-/-}$ and ApoE$^{-/-}$ Akt1$^{-/-}$ mice after 12 weeks of high cholesterol diet were detected by TUNEL and CD68 staining respectively. The data are expressed as the number of TUNEL positive cells per mm^2 cellular lesion area. Bars, 100μm. (**g,h**) Transplantation of bone marrow cells from ApoE $^{-/-}$ or ApoE$^{-/-}$ Akt1 $^{-/-}$ mice into ApoE$^{-/-}$Akt1$^{-/-}$ or ApoE$^{-/-}$mice, respectively, followed by lesion analysis in

aorta (g) and cross sections of aortic sinus (h). Data are mean± S.E.M., from 5 mice (males) in each group*, $p < 0.05$.

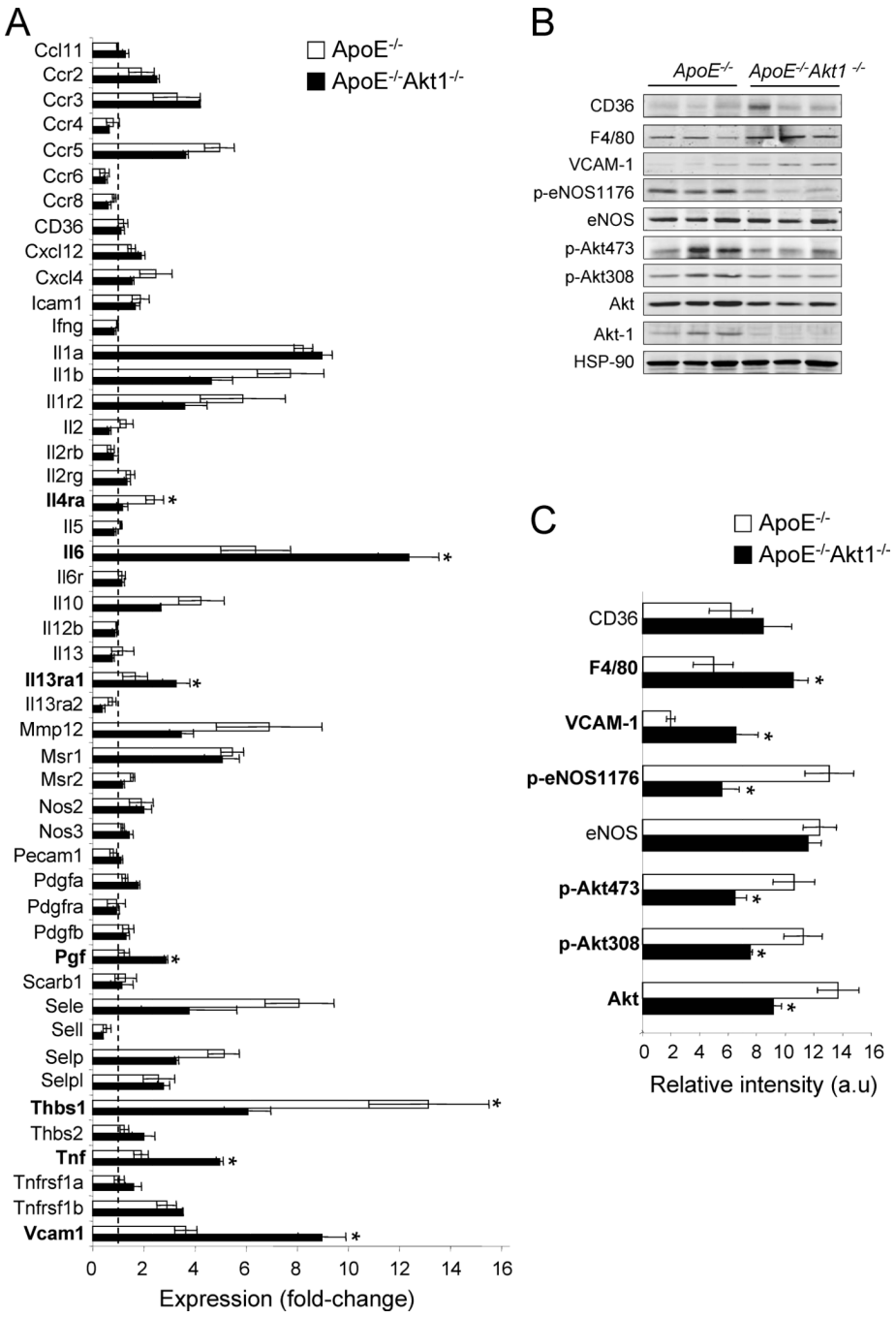

Fig. 6. Loss of Akt1 alters the expression profile of atherosclerosis related genes and proteins

(a) Expression profile of atherosclerosis related genes assessed with PCR Array technology. Three independent arrays were carried out for each condition using iCycler (BioRad). The fold-change for each gene from mice after diet to before diet was calculated. The data represent the mean ± S.E.M. of triplicate simples. Western blot analyses **(b)** and band densitometry **(c)** of CD36, F4/80, eNOS, peNOS-1176, eNOS, Akt, pAkt473, pAkt308 and Akt1 from $Akt1^{+/+}ApoE^{-/-}$ and $Akt1^{-/-}$ $ApoE^{-/-}$ mice feed with high cholesterol diet for 12 weeks. Results from three representative mice are shown for each genotype. The data

represent the mean ± S.E.M. of triplicate samples; *$p < 0.05$ compared with $Akt1^{+/+}$ $ApoE^{-/-}$.

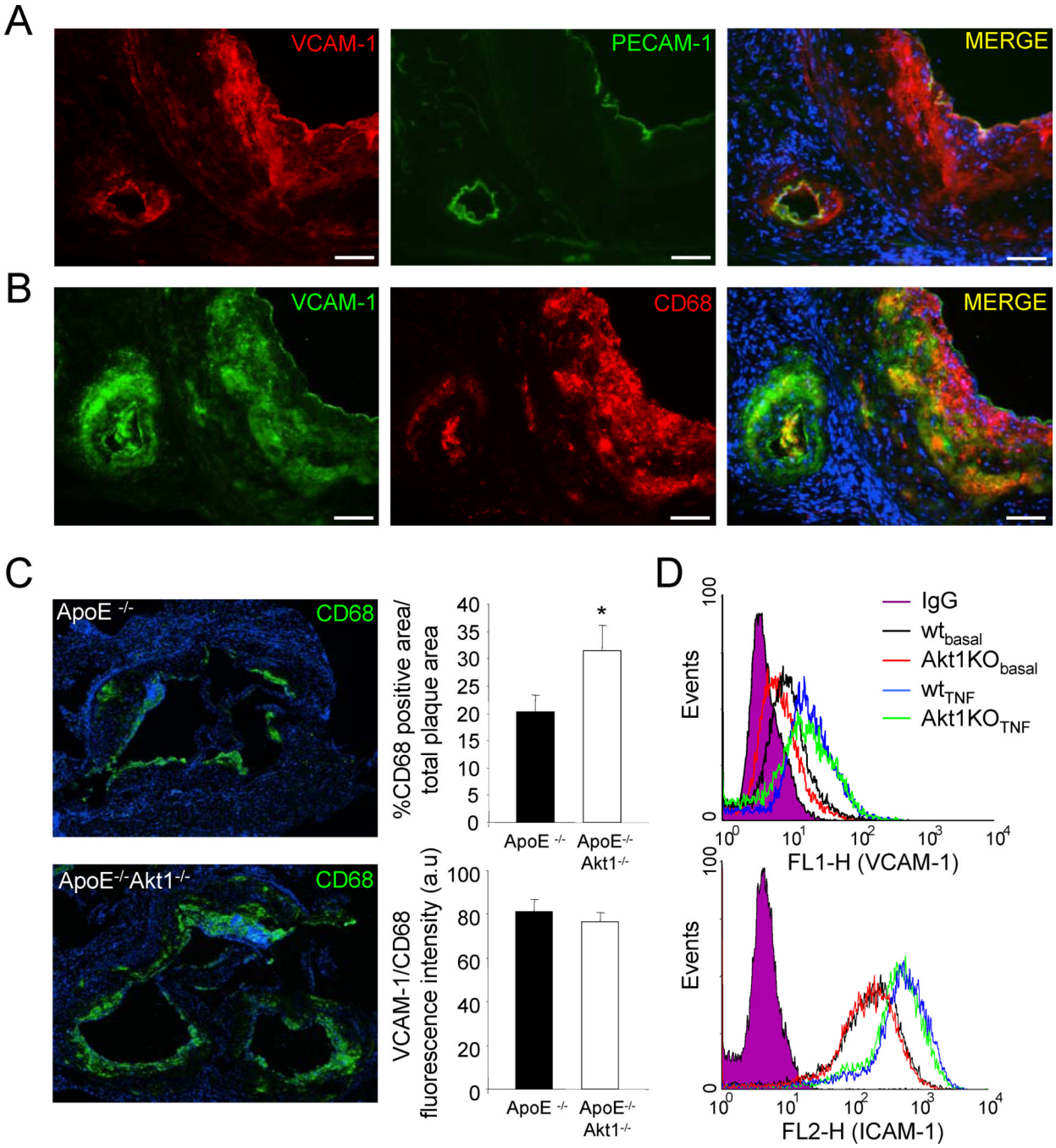

Fig. 7. Increased macrophage infiltration and VCAM-1 expression in the absence of Akt1

(a-b) Representative examples of cross sections from the aortic sinus labelled for VCAM-1, CD68 and PECAM-1. Bars, 100μm. **(c)** CD68 positive macrophages in lesions from ApoE$^{-/-}$ and ApoE$^{-/-}$ Akt1$^{-/-}$ mice after 12 weeks of high cholesterol diet were detected by CD68 staining respectively. The data are quantified as CD68 TUNEL positive area versus total lesion area (upper right panel) and the relative fluorescence intensity of VCAM-1 (red channel) in the CD68 positive area (green channel, bottom right panel). **(d)** VCAM-1 (upper) and ICAM-1 (bottom) expression analysis by flow cytometry in endothelial cells

isolated from WT or Akt1 KO mice that were treated with TNFα for 16h. These data are representative of three separate experiments yielding similar results.